frontiers in
CELLULAR AND INFECTION MICROBIOLOGY

ORIGINAL RESEARCH ARTICLE
published: 01 March 2012
doi: 10.3389/fcimb.2012.00013

Mechanism of *H. pylori* intracellular entry: an *in vitro* study

***H. Liu*[1,2†], *C. Semino-Mora*[1,2†] *and Andre Dubois*[1,2*]**

[1] *Laboratory of Gastrointestinal and Liver Studies, Department of Medicine, Uniformed Services University of the Health Sciences, Bethesda, MD, USA*
[2] *United States Military Cancer Institute, Bethesda, MD, USA*

Edited by:
D. Scott Merrell, Uniformed Services University, USA

Reviewed by:
Richard Peek, Vanderbilt University Medical Center, USA
Karen Guillemin, University of Oregon, USA
Yoshio Yamaoka, Baylor College of Medicine, USA

****Correspondence:***
Andre Dubois, Laboratory of Gastrointestinal and Liver Studies, Department of Medicine, Uniformed Services University of the Health Sciences, 4301 Jones Bridge Road, Bethesda, MD 20814, USA.
e-mail: adubois@usuhs.mil

†H. Liu and C. Semino-Mora have contributed equally to this work.

The majority of *Helicobacter pylori* reside on gastric epithelial cell surfaces and in the overlying mucus, but a small fraction of *H. pylori* enter host epithelial and immune cells. To explore the role of the *nudA* invasin in host cell entry, a Δ*nudA* deletion derivative of strain J99 was constructed and transformants were verified by PCR and by fluorescence *in situ* hybridization. AGS cells were inoculated with either wild type (WT) strain J99 or its Δ*nudA* mutant to determine the fraction of bacteria that were bound to the cells and were present inside these cells using the gentamicin protection assay. We observed no significant difference between either the density of *H. pylori* bound to AGS cell membranes or the density of intracellular *H. pylori*. To further explore this finding, separate chambers of each culture were fixed in glutaraldehyde for transmission electron microscopy (TEM) and immunogold TEM. This addition to the "classical" gentamicin assay demonstrated that there were significantly more intracellular, and fewer membrane-bound, *H. pylori* in WT-infected AGS cells than in Δ*nudA* allele infected cells. Thus, the sum of intracellular *and* membrane-bound *H. pylori* was similar in the two groups. Since no other similar TEM study has been performed, it is at present unknown whether our observations can be reproduced by others Taken together however, our observations suggest that the "classical" gentamicin protection assay is not sufficiently sensitive to analyze *H. pylori* cell entry and that the addition of TEM to the test demonstrates that *nudA* plays a role in *H. pylori* entry into AGS cells *in vitro*. In addition, deletion of the invasin gene appears to limit *H. pylori* to the AGS cell surface, where it may be partly protected against gentamicin. In contrast, this specific environment may render *H. pylori* more vulnerable to host defense and therapeutic intervention, and less prone to trigger normal immune, carcinogenic, and other developmental response pathways.

Keywords: *H. pylori*, intracellular, adhesion, adhesin, *nudA*, electron microscopy

INTRODUCTION

The pathogenicity of many bacteria colonizing the gastrointestinal tract often depends on their ability to gain access to cells that are normally non-phagocytic. *Helicobacter pylori* colonizes the stomach of over half the world population and is the main cause of peptic ulcer disease and gastric cancer. It often is considered to be a non-invasive pathogen present only in the lumen of the stomach and attached to gastric epithelial cells although a number of *in vivo* and *in vitro* studies have demonstrated that *H. pylori* is in fact invasive (Dubois and Berg, 1997; Engstrand et al., 1997; Amieva et al., 2002; Semino-Mora et al., 2003; Necchi et al., 2007). In addition, *H. pylori* can repopulate the extracellular environment after elimination of extracellular bacteria with gentamicin, suggesting it may be considered a facultative intracellular bacterium (Amieva et al., 2002). Finally, *H. pylori* may be present inside metaplastic, dysplastic, and neoplastic epithelial cells (Semino-Mora et al., 2003). The multiplicity of these observations and the fact that various methods were used to reach the same conclusions strongly support their validity.

Bacterial invasion of eukaryotic cells appears to be mediated by Nudix enzymes, initially called MutT because *E. coli* MutT was the first Nudix hydrolase to be described (Maki and Sekiguchi, 1992). The *Bartonella bacilliformis* Nudix hydrolase, encoded by the *ialA* gene, was shown to be associated with the ability to invade human erythrocytes using the gentamicin assay complemented by transmission electron microscopy (TEM; Mitchell and Minnick, 1995). Similarly, invasion of human brain microvascular endothelial cells by *E. coli* is accompanied by increased expression of the K1 ortholog *ygdP* and the early stages of infection of infection by *Rickettsia prowazekii* ortholog is temporarily accompanied by an increased transcription of the *invA* gene (Lundin et al., 2003). Finally, the *invA* gene was highly conserved in protein sequence and present in all tested members of the pathogenic *Leptospira* species (Luo et al., 2011).

Helicobacter pylori appears to be a suitable system to study the biological role of Nudix hydrolases since the NudA protein is the only dinucleoside polyphosphate hydrolase homolog present in the two first strains that were sequenced (Tomb et al., 1997; Alm et al., 1999). J99 *H. pylori* harbors one Nudix hydrolase ortholog, *Nud*ix hydrolase *A*, *nudA*, with the gene numbers JHP1149 (Alm et al., 1999), 26,695 strain harbors HP1228 (named *invA*; Tomb et al., 1997), and a GenBank search showed that a *nudA* gene is present in 30 additional completely sequenced *H. pylori* strains.

Due to the functional heterogeneity within this group of proteins, *H. pylori* NudA may be involved in (1) DNA repair, (2) oxidative stress and/or heat shock response, or (3) bacterial invasion of epithelial cells through degradation of toxic substances induced during invasion (Lundin et al., 2003). These authors describe the enzymatic function of the Nudix hydrolase NudA in *H. pylori* and they constructed a *nudA* insertion mutant to determine the biological role of this protein. Using the classical gentamicin protection assay (Kwok et al., 2002), the authors found no quantifiable differences in invasion frequency by the *NudA H. pylori* J99 strain mutant compared to WT but they did not show the data (Lundin et al., 2003). Their conclusion was that they found no supportive evidence for a role for the NudA protein in *H. pylori* invasion of AGS cells, although they warned that this could be due to the fact that complete eradication of extracellular bacteria is rarely obtained in the gentamicin protection assay (Amieva et al., 2002). They also concluded that the gentamicin assay of AGS cells invasion by *H. pylori* lacked the sensitivity needed to demonstrate differences in their experimental setup.

In the present study, we examined the role of *H. pylori* invasin J99 NudA in *H. pylori* entry into gastric epithelial cells. To this effect, we generated a Δ*nudA* allele of strain J99 in which *nudA* was replaced by a chloramphenicol resistance gene (CAM). Absence of the *nudA* gene was verified and the effect of this deletion on colonization was studied *in vitro* using the classical gentamicin assay aided by ultrastructural studies as used by others (Mitchell and Minnick, 1995).

MATERIALS AND METHODS

CONSTRUCTION OF A Δ*nud*a ALLELE MUTANT

A Δ*nudA* allele in which *nudA* was replaced by the chloramphenicol resistance cassette (CamR) was constructed from a low-pass isolate of the J99 strain (kindly provided by Dr. R. Peek) and using a PCR method as reported earlier (Chalker et al., 2001; Tan and Berg, 2004). Culture of single colony isolates in the presence of chloramphenicol was then used to select for Δ*nudA* alleles carrying CAM. Genomic DNA was extracted from fresh *H. pylori* isolates using the QIAamp DNA Mini Kit (Qiagen, Valencia, CA, USA) and this DNA was used for confirmation of the mutant. Presence of CAM and absence of *nudA* in single colony isolates was then verified using PCR (**Figure 1**) and fluorescence *in situ* hybridization (**Figure 2**). The CamR and *nudA* sequences were confirmed using BigDye® Terminator v3.1 Cycle Sequencing Kit (Applied Biosystems Inc.).

GENTAMICIN PROTECTION VIABILITY ASSAY EXPERIMENTAL DESIGN

Human gastric adenocarcinoma cell line AGS was purchased from ATCC and maintained in 5% CO_2 atmosphere in Dulbecco's Modified Eagle Medium (DMEM, Gibco/BRL) supplemented with 10% fetal bovine serum (FBS, Gibco/BRL) for 2 days in 10-cm dishes for culture and then in 12-well plates (5×10^4/well) for gentamicin protection assay and four- or eight-chamber slides (Nunc Lab-Tek II Chamber Slide System)[1] for light and TEM.

[1] www.thermofisher.com

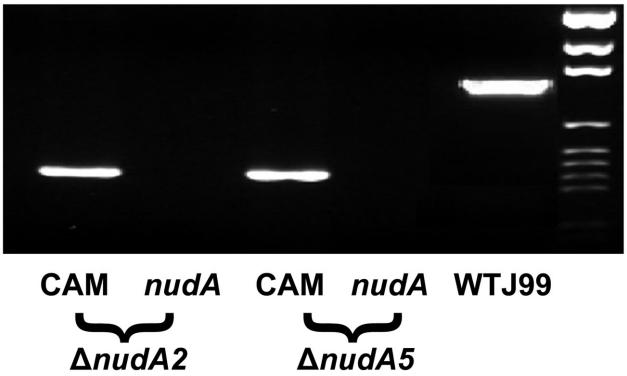

FIGURE 1 | Verification of post-transformation bacterial DNA in the Δ*nudA* allele PCR products on agarose gel. Two pairs of primers were designed for verification of post-transformation of bacterial transformed with Δ*nudA* allele PCR products. One pair was specific for *nudA* and the other pair was specific for the CamR gene. The wild type strain J99 PCR product was used as positive control. The figure illustrates that the *nudA* gene was present only in wild type strain J99 but absent in *nudA* mutant strains while the CamR gene was present in *nudA* mutant strains but not in the wild type.

AGS cells were grown to monolayer in two groups of four plates or chambers and a similar number of *H. pylori* J99 WT and of the Δ*nudA* mutant was inoculated into each group of plates/chambers (4×10^3 *H. pylori*/cell). Two plates and chambers were cultured for 6 h, used as negative control, and infected with *H. pylori* plus 200 μg/ml gentamicin (**Figure 3**; controls, left side) for 12 h. One of the two plates or wells was treated with 0.1% saponin for 15 min and then cultured for *H. pylori*. Saponin was used to permeabilize AGS cell membranes by penetrating the cholesterol monolayer and forming holes or pits (7–9 nm) that is believed to allow *H. pylori* to exit from AGS cells and be cultured (Bangham et al., 1962; Kwok et al., 2002). The remaining two plates and chambers were used to study *H. pylori* binding and cell invasion (**Figure 3**; right side) and were infected with *H. pylori* for 6 h. One of the two plates or chambers was treated with gentamicin, cultured for 12 h, treated with saponin for 15 min, and then plated on BAP for colony counting or fixed with formaldehyde or glutaraldehyde (see below).

CALCULATION AND NORMALIZATION OF *H. pylori* ENTERING INTO, OR BINDING TO, AGS CELLS

Counting of *H. pylori* can be done via OD measurement, but this method is not precise or very accurate. Instead, we counted the number of colonies used for plates and well inoculation by plating and culturing the *H. pylori* suspension for 3 days. Colony counting after treatment with and without gentamicin and saponin was then determined by culturing *H. pylori* on plates and then expressing colonization in each compartment as the percentage of *H. pylori* inoculated onto the plates.

MORPHOLOGY AND MORPHOMETRY USING FLUORESCENCE *IN SITU* HYBRIDIZATION AND TRANSMISSION ELECTRON MICROSCOPY

Tissue culture chamber glass slides from each of the four groups were treated using one of the following methods.

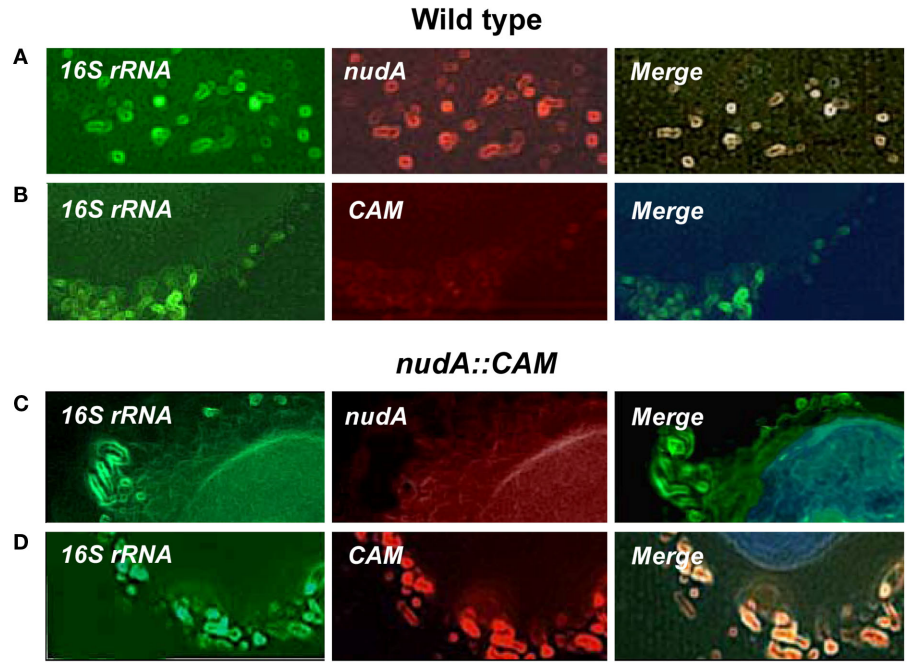

FIGURE 2 | Illustration of the expression of *H. pylori 16S rRNA, nudA,* and chloramphenicol resistance cassette (CAM) in AGS cells infected with *H. pylori* J99 WT (A,B) and ΔnudA allele (C,D). (A) *16S rRNA* and *nudA* expression and complete merge of the two genes (green, red, and yellow, respectively). **(B)** *16S rRNA* expression, no expression of CAM, and no merge. **(C)** *16S rRNA* expression, no expression of *nudA,* and no merge. **(D)** *16S rRNA* and CAM expression and complete merge of the two genes (green, red, and yellow, respectively). Original magnification: 1,000×.

For *H. pylori* dual fluorescence *in situ* hybridization (FISH), glass chambers were immediately fixed in 4% formaldehyde for 24 h and then processed using probes designed specifically for *H. pylori 16S rRNA* (digoxigenin–FITC) and *nud*A (Biotin–Texas red) or *16S rRNA* (digoxigenin–FITC) and CAM (biotin–Texas Red) were designed and synthesized as reported (Liu et al., 2008). Control of method was performed as described (Semino-Mora et al., 2003). Chambers were observed using a Nikon Eclipse 80i microscope and pictures were taken using a DS-Qi1MC Nikon camera (**Figure 2**).

For TEM, plastic chamber slides with four wells were immediately fixed in 2.5% glutaraldehyde for 24 h, the AGS cells were scraped and transferred to Eppendorf tubes, post-fixed in 1% osmium tetroxide at 4°C, and processed as reported until embedding in Spurr Low Viscosity Kit[2] to obtain epoxy blocks at 70°C (Semino-Mora et al., 2003). Semi-thin (0.5 μm) sections were stained with toluidine blue and observed by light microscopy using an Eclipse E800 Nikon interfaced with a QCapture digital camera (Micropublisher 5.0, Burnaby, BC, Canada). Grids with thin sections (500 A) were prepared, stained with uranyl acetate and lead citrate, and then observed using a Philips CM100 transmission electron microscope at 80 kV (Biomedical Instrumentation Center, USUHS).

For TEM immunohistochemistry with pre-embedding, plastic chamber slides with eight chambers each were processed inside each chamber slide (*in situ* method; Tanner et al., 1996). Immunogold was performed using rabbit anti-*H. pylori* (NeoMarkers, Fremont, CA, USA) and immunogold-labeled secondary antibodies (18 nm colloidal gold, goat anti-rabbit IgG; Jackson ImmunoResearch, West Grove, PA, USA) and after intermediate steps were embedded in Spurr embedding. In other experiments, dual immonogold pre-embedding was performed using both rabbit anti-*H. pylori* and mouse anti-VacA antigen IgG anti-VacA (Secondary 18 nm colloidal gold, goat anti-rabbit IgG, and 11 nm colloidal gold, respectively, Jackson, InmunoResearch, West Grove, PA, USA). After polymerization, the flat resin blocks were removed by peeling them away from each chamber, mounted in blank mold, and cut in ultramicrotomy. Sections were stained only with uranyl acetate. Control of method was performed in AGS cells infected with WT or Δ*nudA*, were treated with PBS instead of the anti-*H. pylori* first antibody, and were processed as described above for pre-embedding immunogold method. Control of *H. pylori* detection with immunogold with pre-embedding was performed using chamber slides with non-infected AGS cells treated as described above. Importantly, all positive and negative controls were positive and negative, respectively.

A Philips CM100 transmission electron microscope was used at 80 kV for the analysis (Biomedical Instrumentation Center, USUHS) and negatives and photographs were processed. Visibility of colloidal gold particles in the pictures was enhanced using color burn option (Adobe Photoshop 7.0.1) that examines the color information in each channel and darkens the base color to reflect the blend color by increasing the contrast between the two). Nickel

[2]www.polysciences.com

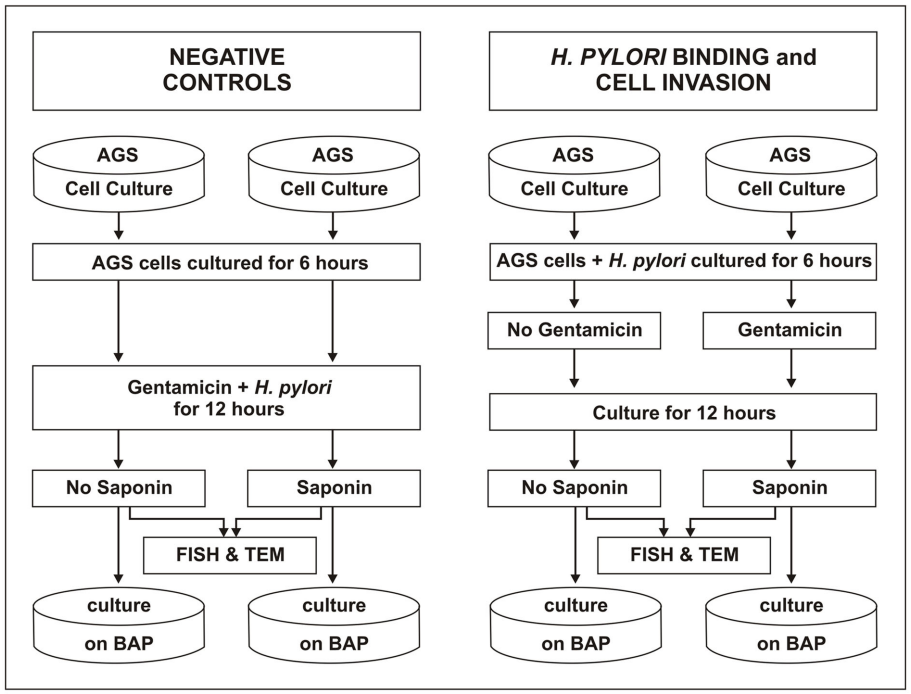

FIGURE 3 | Experimental design of the gentamicin protection assay. AGS cells were prepared to grow to monolayer in 8 wells in a 12-well plate (four wells for WT strain J99 and four wells for Δ*nudA* mutant. Each strain was inoculated into the four AGS cell types. Two wells (on the left) were designed as negative control of gentamicin treatment as it was added to *H. pylori* suspension when inoculated to the cells, and then treated with or without saponin after 12 h inoculation. A third well was used for measurement of *H. pylori* bound to cell membranes in the conditions without gentamicin and saponin. The last well was designed for measurement of *H. pylori* invasion into the cell with gentamicin and saponin added. The chamber slides prepared for morphologic observation were exactly the same as above.

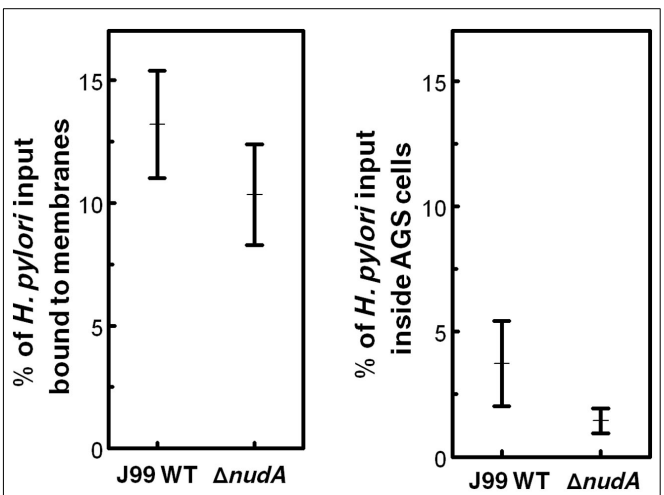

FIGURE 4 | *Helicobacter pylori* NudA invasin and AGS cell entry determined using the "classical" gentamicin protection assay. Values are Means ± SEM. Left panel shows that the density of *H. pylori* bound to AGS cell membranes and expressed as the percentage of bacteria inoculated into the AGS monolayer was not significantly different in WT J99 and the Δ*nudA* mutant ($p = 0.35$). Right panel shows that the density of intracellular *H. pylori* expressed as the percentage of bacteria inoculated into the AGS monolayer was not significantly different in WT J99 and the Δ*nudA* mutant after saponin treatment ($p = 0.23$).

grids with five sections were counted at 10,500× in a selection of three mesh areas at a low magnification (2,600×). The number of cells was around 25–30 cells/mesh and two fields were counted in each mesh.

Morphometry

Qualitative fluorescence light microscopy ranged from 0 (negative reaction) to 4 (maximum red, green and yellow). Quantitative bright light microscopy of semi-thin sections stained with toluidine blue was used to count the density of *H. pylori* located in the extracellular or intracellular compartments, or attached to the cellular membrane of AGS cells using an intraocular grid (Semino-Mora et al., 2003). Three random fields were counted with 1,000× magnification (cell range 77–115/field, mean 96 ± 3/field; total cells counted 300 cells). Elongated cells with hummingbird phenotype were counted as hallmark of infection and compared to normal round cells in uninfected controls (no infection; Schneider et al., 2008).

Quantitative pre-embedding immunogold TEM was performed by counting electron dense gold particles specifically tagging *H. pylori* located in the extracellular, intracellular, and within cell membrane compartments (Tanner et al., 1996). Three grids of each experiment were analyzed as follows: five sections mounted in the nickel grid were counted at 14,000×. Three meshes were selected at low magnification (2,600×) and two fields were counted in each mesh (number of cells counted

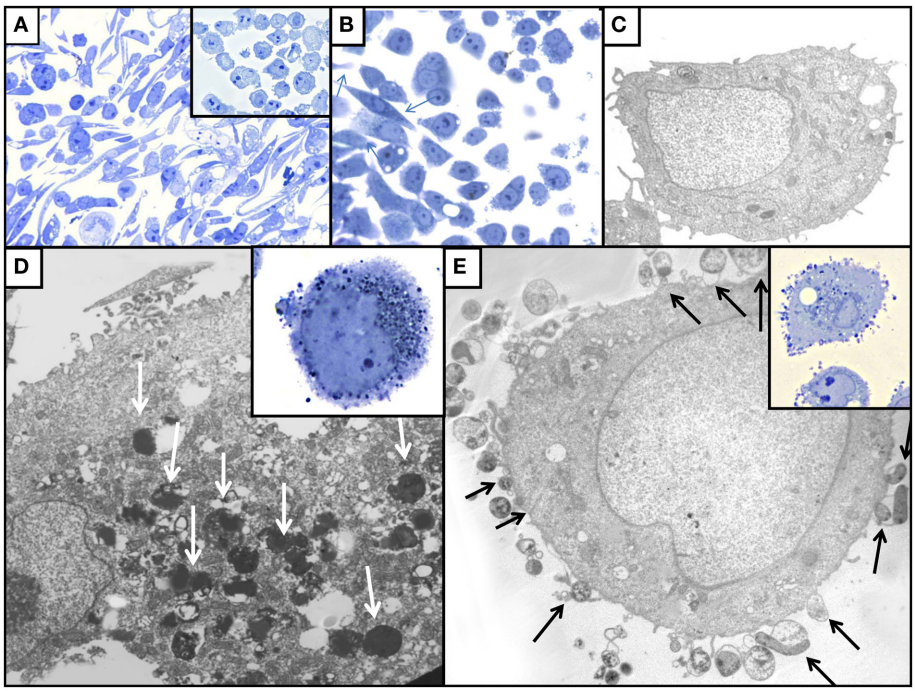

FIGURE 5 | Illustration of the effect of *H. pylori* colonization on AGS cell monolayers in toluidine blue stained sections [(A,B) inserts of (A,D,E)] and by TEM (C,D,E). (A) WT-infected AGS cells; note the presence of numerous elongated hummingbird cells that are absent among control uninfected AGS cells (insert). **(B)** AGS cells infected with Δ*nudA* allele, illustrating that fewer elongated AGS cells (arrows) are present that in WT-infected cells. **(C)** TEM of uninfected AGS cell with normal ultrastructural aspect. **(D)** TEM of AGS cell infected with J99 WT *H. pylori*; note intracellular *H. pylori* (white arrows). **(E)** TEM of AGS cell infected with Δ*nudA* allele; note *H. pylori* attached to AGS cell (arrows); insert shows the numerous Δ*nudA H. pylori* attached to AGS cell and relatively few intracellular bacteria. Original magnification of toluidine blue stained pictures **(A)**: 400×; **(B)** and insert of **(A)**: 1,000×; inserts of **(D,E)**: 1,000×. Original magnification of TEM pictures: **(C)**: 9,800×; **(D)**: 32,500×; **(E)**: 26,000×.

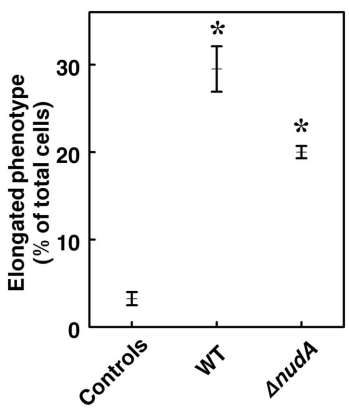

FIGURE 6 | Percentage of AGS cells with elongated ("hummingbird") phenotype in cells infected with WT J99 and Δ*nudA H. pylori* compared to control uninfected cells. Values are Means ± SEM. The percentage of cells with abnormal phenotype is higher in both types of infection (*$p < 0.001$), and also significantly higher in infection with WT *H. pylori* than with the ΔnudA mutant ($p < 0.01$).

∼25–30 cells/mesh) at higher magnification. A 17.5 cm × 23 cm transparent sheet grid with vertical and horizontal lines 1-cm apart with 374 intersections was placed on each micrograph printed on multi contrast Agfa paper. The point counting method was used to calculate the number of immunogold-tagged *H. pylori* as coincidences between bacterial electron dense gold particles and point grid intersections and expressed as a fraction of the total points intersections (Olivero et al., 1990).

STATISTICAL ANALYSIS

Data are reported as mean ± SEM. Comparisons were performed using one way analysis of variance and subsequent *t*-tests.

RESULTS

In a "classical" gentamicin protection assay, the density of *H. pylori* bound to AGS cell membranes and expressed as the percentage of bacteria inoculated into the AGS monolayer was not significantly different in WT J99 and the Δ*nudA* mutant (**Figure 4**, left panel). Similarly, the density of intracellular *H. pylori* expressed as the percentage of bacteria inoculated into the AGS monolayer was not significantly different in WT J99 and the Δ*nudA* mutant after saponin treatment (**Figure 4**, right panel).

The addition of FISH and ultrastructural techniques to the "classical" gentamicin protection assay used in our study allowed a detailed analysis of the precise location of *H. pylori* in relation to the AGS cells, as was observed in the case of invasion of erythrocytes by *B. bacilliformis* (Mitchell and Minnick, 1995). Light microscopy performed on sections stained with toluidine

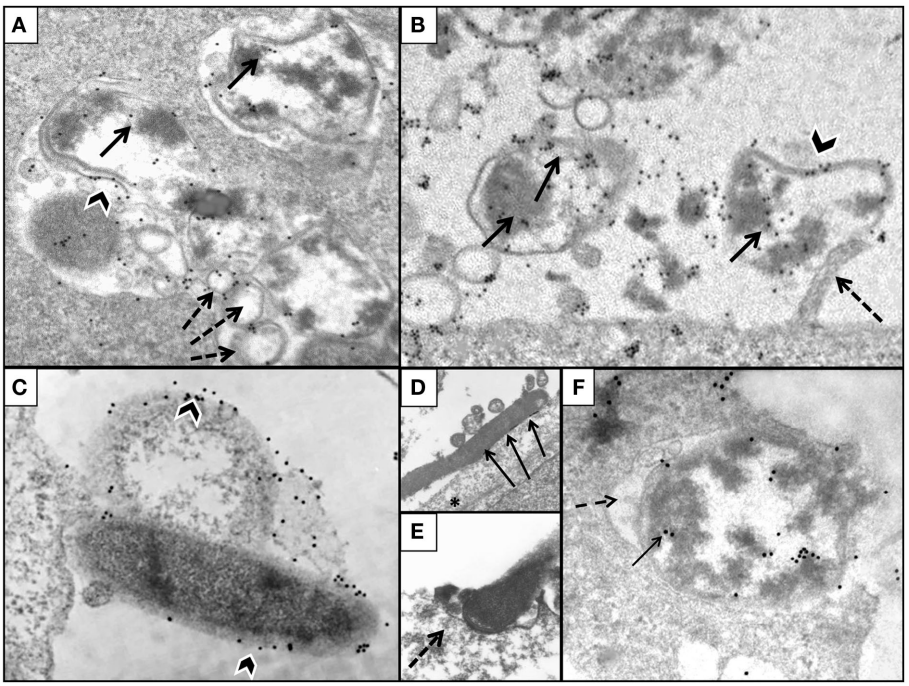

FIGURE 7 | Illustration of AGS cells with pre-embedded *H. pylori* immunogold. (A) AGS cell infected with *H. pylori* WT demonstrating intracellular presence of bacteria located inside vacuoles (gold marked bacterial wall, black arrowhead); note gold particles tagging *H. pylori* cytoplasm (arrow) and spherical membrane vesicles (dashed arrows). **(B)** Δ*nudA* allele with numerous bacteria labeled with gold (arrows) in close association with cell membrane; one of the bacteria is attached to cell pedestal (dashed arrow). **(C)** Mature and coccoid Δ*nudA* allele in close association with AGS cell membrane; note bacterial membrane is tagged with gold (arrowheads). **(D)** Δ*nudA* allele in early stage of adhesion to AGS cell; note multiple fusions between membranes of bacterium and AGS cell (arrows). **(E)** Higher magnification of "zipper-like" Δ*nudA* allele allele entry into AGS cell; note "cup formation" (dashed arrows) identifying *H. pylori* and AGS cell membranes fusing together during internalization. **(F)** Δ*nudA* allele almost completely englobed within invagination of AGS cell membrane; note that this fusion is accompanied by the presence of filamentous strands (fibrils), dense round spheres, vesicles, and amorphous deposits in the space between the membranes of the bacterium and AGS cell (dashed arrow). Immunogold-tagged bacterium (solid arrow) Original magnification **(A–C)**: 41,000×; **(D)**: 24,500×; **(E)**: 32,500×; **(F)**: 41,000×.

blue demonstrated that elongated cells ("hummingbird" phenotype) were more frequently observed in AGS cells infected with WT J99 strain (**Figures 4**, left panel and **5**) than in control uninfected cells ($p < 0.001$; **Figure 5A** insert and **Figure 6**). In Δ*nudA* allele infected cells, most *H. pylori* are associated with the membrane area and cell invasion is minimal but there still are significantly more elongated cells that in the absence of infection ($p < 0.01$) but less than with J99 WT (**Figures 5B** and **6**; $p < 0.01$). Remaining cells are round or square. These results suggest that intracellular *H. pylori* are responsible for the hummingbird transformation of AGS cell in WT-infected cells compared to control uninfected cells, but that membrane associated *H. pylori* may also play a role in the formation of elongated cells.

Transmission electron microscopy indicated that more bacteria were present inside J99 WT-infected AGS cells (**Figure 5D**) than in Δ*nudA* allele infected cells and that more bacteria were closely associated with cell membranes in the latter cells (**Figure 5E**). After infection with J99 WT isolates, more bacteria were observed inside AGS cells (**Figure 5D**) than with the Δ*nudA* allele, but more bacteria were observed within the external surface of AGS cell membranes with the Δ*nudA* allele (**Figure 5E**). More intracellular *H. pylori* were observed inside AGS cell vacuoles than in direct contact with the cytosol, free in the cytoplasm (66.7 vs. 16.7%), the remaining *H. pylori* were partly in a vacuole and partly free in the cytoplasm.

Morphometry of TEM thin sections confirmed these findings, demonstrating that the number of AGS cells infected with J99 WT was significantly greater than with Δ*nudA* infection (39.8 ± 2.8 vs. 12.3 ± 2.2%, respectively; $p < 0.001$). In addition, there were significantly more intracellular *H. pylori* in WT-infected AGS cells than in Δ*nudA* allele infected cells (15.4 ± 2.1 vs. 6.9 ± 1.9; $p < 0.01$; **Figure 5D**), and more *H. pylori* were attached to AGS cells infected with Δ*nudA* allele (8.1 ± 2.6 vs. 0.3 ± 0.2, respectively; $p < 0.01$; **Figure 5E**). Importantly, the number of extracellular *H. pylori* not attached to the plasma membrane was similar in those two groups (4.2 ± 0.9 vs. 5.3 ± 2.0 respectively).

The TEM pre-embedding immunogold method with pre-embedding of *H. pylori* infected AGS cells was more effective to detect hidden epitopes than post-embedding method as reported (Tanner et al., 1996). The use of this method confirmed observations obtained with light microscopy that more WT *H. pylori* were intracellular than in Δ*nudA* allele infection and that more Δ*nudA* allele were attached to AGS cell membranes than in WT infection. In addition, intracellular *H. pylori* WT located inside vacuoles had gold-tagged bacterial walls, cytoplasm (**Figure 7A**), and outer membrane vesicles containing *H. pylori* VacA (**Figure 8**;

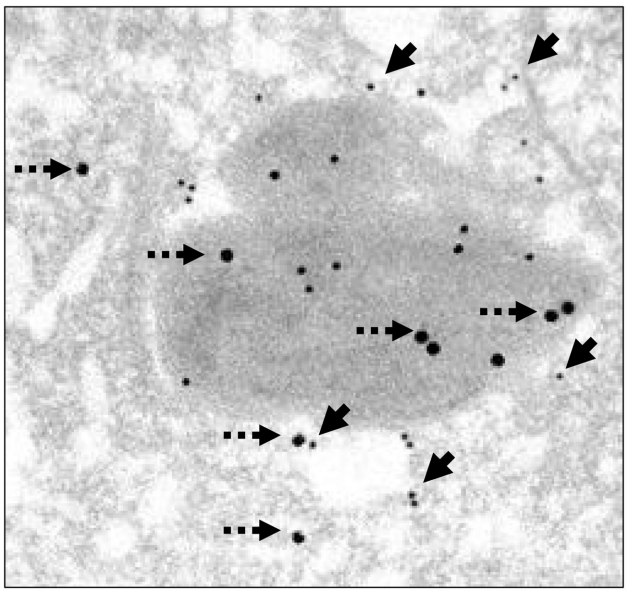

FIGURE 8 | Illustration of AGS cells with intracellular *H. pylori* WT with *H. pylori* and VacA immunogold. AGS cell infected using a dual pre-embedding immunogold (*H. pylori* gold 18 nm and VacA-gold 11 nm) demonstrating the presence of 18 nm *H. pylori* gold particles (dashed arrow) and 11 nm VacA-gold particles in cytoplasm, in the cell membrane, in membrane vesicles, and in the AGS cell. Original magnification 71,000×.

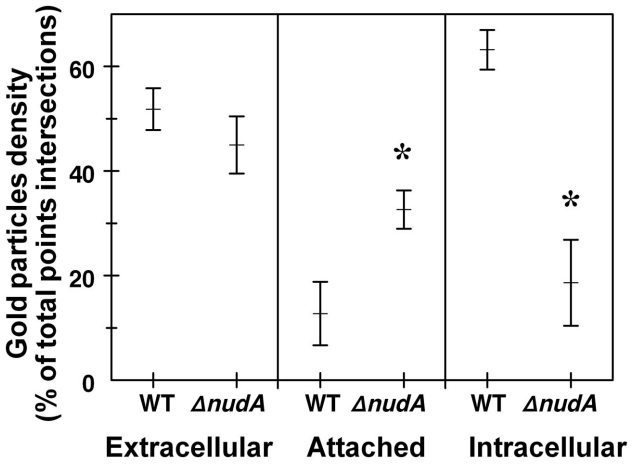

FIGURE 9 | Role of *H. pylori* NudA invasin in AGS cell entry determined using the gentamicin protection assay aided by TEM and anti-*H. pylori* antibody immunogold. *H. pylori* density is expressed as the percentage of total points intersections that were immunogold-positive (see Materials and Methods). Values are Means ± SEM. Left panel shows that the extracellular density of *H. pylori* WT and Δ*nudA* were not significantly different. In contrast, the middle and right panels show that the density of WT *H. pylori* attached to AGS cell membranes was significantly lower than that of the Δ*nudA* mutant (*$p < 0.01$) and the opposite relation for the density of intracellular *H. pylori* (*$p < 0.01$).

Beveridge, 1999; Fiocca et al., 1999; Viala et al., 2004). Similarly, immunogold-labeled Δ*nudA* allele *H. pylori* were closely associated with AGS cell membranes, either attached to cell pedestals (**Figure 7B**) or to AGS cell membranes (**Figure 7C**) or undergoing diverse stages of "zipper-like" entry into AGS cell (**Figures 7D–F**; Noach et al., 1994; Papadogiannakis et al., 2000) Morphometric quantification of these observation demonstrated that most WT *H. pylori* and very few Δ*nudA* allele *H. pylori* were present inside the AGS cells and that the opposite was observed regarding attachment to AGS cell membranes (**Figure 9**; $p < 0.01$).

DISCUSSION

A major finding of the present study was that *H. pylori* invasin appears to play a complex role in the entry of the bacterium into AGS cells *in vitro* if the "classical" gentamicin protection assay is complemented by morphology and morphometry. We first confirmed the previous report that no quantifiable differences were found when using the gentamicin protection assay to compare the invasion frequency of *H. pylori* wild type (WT) with that of a Δ*nudA* mutant in AGS cells allele (Lundin et al., 2003). The authors of the report attributed their observation to the fact that the sensitivity of the "classical" assay may not be sufficient to demonstrate differences in invasion capacity, and this lack of sensitivity may be due to the fact that complete killing of extracellular bacteria is rarely obtained (Amieva et al., 2002). In the present study, light and TEM morphology and morphometry of AGS cells demonstrated that a majority of *H. pylori* were closely associated with cell membranes after infection with the Δ*nudA* allele whereas most WT J99 bacteria were inside the cells. The TEM immunogold observations confirm this observation (**Figures 7** and **9**; $p < 0.01$) and strongly indicate that this difference demonstrates that NudA plays a biologically significant role in *H. pylori* entry into host cells.

The present study also provides precise information on *H. pylori* invasion and bacterial cell entry, demonstrating that *H. pylori* Δ*nudA* allele appears to be unable to proceed beyond the initial attachment to cell membranes that characterize the zipper-like mechanism of *H. pylori* cell entry (Griffin Jr. et al., 1975; Kwok et al., 2002). In contrast, J99 WT *H. pylori* rapidly proceeded from attachment to engulfment and internalization where it was found mostly inside vacuoles formed within AGS cells and, to a lesser extent, free in the cytoplasm. Our observations that gold-tagged outer membrane vesicles containing VacA were closely associated with intracellular *H. pylori* (**Figure 8**) demonstrates that *H. pylori* virulence factors and peptidoglycan may be delivered directly into the AGS cell cytoplasm (Blanke and Ye, 2001; Kaparakis et al., 2010) and suggests an important pathogenic role for cell invasion. This finding is similar to the observation that *H. pylori* releases small vesicles from its outer membrane by a process similar to the release of membrane vesicles by many other bacterial pathogens (Fiocca et al., 1999). The production of these vesicles may represent an important mechanism for bacterial pathogens to modulate their environment within the host and perhaps cause diseases. Finally, separate experiments showed that the *H. pylori nudA* (invasin homolog) gene is well expressed only when *H. pylori* is attached to or inside host cells and that it was closely associated with β1-integrin (Semino-Mora, unpublished).

An additional study of this highly relevant question demonstrated that the extent of adherence and internalization of *H. pylori* by AGS cells increased continuously for at least 12 h, and that a similar number of *H. pylori* were internalized by, and adherent to, AGS cells (Kwok et al., 2002) suggesting again that the "classical" gentamicin assay determines the sum of internalized and adherent *H. pylori*. However, the construction of a Δ*nudA* mutant performed in this study may have modified the expression of neighboring genes that might affect cell invasion. Since genetic complementation of the mutation and restoration of the WT phenotype was not performed as a control, our observations do not exclude the possibility that the internalization defect we observed is related to factors other than the *nudA* gene.

Helicobacter pylori invasiveness is important because intracellular bacteria are more resistant to antibiotic treatment and to immune attack by humoral antibodies. In addition, invasive organisms frequently cause common and severe diseases (Isberg et al., 1987) through mechanisms that are presently unknown (Dubois and Boren, 2007). Importantly, it is now recognized that bacteria invading host cells can induce formation of autophagic vacuoles within macrophages and dendritic cells where they can multiply, interfere with MHC class II surface expression, impair antigen presentation, and immunological defenses (Wang et al., 2009). In turn, these mechanisms would explain persistence of the infection and the various diseases caused by *H. pylori*.

In conclusion, our observations strongly indicate that deletion of the invasin gene limits *H. pylori* to the AGS cell surface, where it appears to be partially protected against gentamicin (Corthesy-Theulaz et al., 1996). In this site, however, it may be more vulnerable to host defense or therapeutic intervention than if intracellular, and less prone to trigger normal immune, carcinogenic, or other developmental response pathways. These data suggest that *H. pylori* invasin gene is important for the rare, but we propose potentially biologically significant, uptake of *H. pylori* by host cells.

ACKNOWLEDGMENTS

We thank Douglas Berg for stimulating discussions and for helpful comments on the results of these experiments and Donald F. Sellitti for reviewing the manuscript. This work was supported in part by NIH grant CA082312.

REFERENCES

Alm, R. A., Ling, L. S., Moir, D. T., King, B. L., Brown, E. D., Doig, P. C., Smith, D. R., Noonan, B., Guild, B. C., deJonge, B. L., Carmel, G., Tummino, P. J., Caruso, A., Uria-Nickelsen, M., Mills, D. M., Ives, C., Gibson, R., Merberg, D., Mills, S. D., Jiang, Q., Taylor, D. E., Vovis, G. F., and Trust, T. J. (1999). Genomic-sequence comparison of two unrelated isolates of the human gastric pathogen *Helicobacter pylori*. *Nature* 397, 176–180.

Amieva, M. R., Salama, N., Tompkins, L. S., and Falkow, S. (2002). *Helicobacter pylori* enter and survive within multivesicular vacuoles of epithelial cells. *Cell. Microbiol.* 4, 677–690.

Bangham, A. D., Horned, R. W., Glauert, A. M., Dingle, J. T., and Lucy, J. A. (1962). Action of saponin on biological cell membranes. *Nature* 196, 952–955.

Beveridge, T. J. (1999). Structures of Gram-negative cell walls and their derived membrane vesicles. *J. Bacteriol.* 181, 4725–4733.

Blanke, S. R., and Ye, D. (2001). "Alternative mechanisms of protein release," in *Helicobacter pylori: Physiology and Genetics*, eds H. L. T. Mobley, G. L. Mendz, and S. L. Hazell (Washington, DC: ASM Press) , 1–14.

Chalker, A. F., Minehart, H. W., Hughes, N. J., Koretke, K. K., Lonetto, M. A., Brinkman, K. K., Warren, P. V., Lupas, A., Stanhope, M. J., Brown, J. R., and Hoffman, P. S. (2001). Systematic identification of selective essential genes in *Helicobacter pylori* by genome prioritization and allelic replacement mutagenesis. *J. Bacteriol.* 183, 1259–1268.

Corthesy-Theulaz, I., Porta, N., Pringault, E., Racine, L., Bogdanova, A., Kraehenbuhl, J. P., Blum, A. L., and Michetti, P. (1996). Adhesion of *Helicobacter pylori* to polarized T84 human intestinal cell monolayers is pH dependent. *Infect. Immun.* 64, 3827–3832.

Dubois, A., and Berg, D. E. (1997). The nonhuman primate model for *H. pylori* infection. *Methods Mol. Med.* 8, 253–269.

Dubois, A., and Boren, T. (2007). *Helicobacter pylori* is invasive and it may be a facultative intracellular organism. *Cell. Microbiol.* 9, 1108–1116.

Engstrand, L., Graham, D., Scheynius, A., Genta, R. M., and El Zaatari, F. (1997). Is the sanctuary where *Helicobacter pylori* avoids antibacterial treatment intracellular? *Am. J. Clin. Pathol.* 108, 504–509.

Fiocca, R., Necchi, V., Sommi, P., Ricci, V., Telford, J., Cover, T. L., and Solcia, E. (1999). Release of *Helicobacter pylori* vacuolating cytotoxin by both a specific secretion pathway and budding of outer membrane vesicles. Uptake of released toxin and vesicles by gastric epithelium. *J. Pathol.* 188, 220–226.

Griffin, F. M. Jr., Griffin, J. A., Leider, J. E., and Silverstein, S. C. (1975). Studies on the mechanism of phagocytosis. I. Requirements for circumferential attachment of particle-bound ligands to specific receptors on the macrophage plasma membrane. *J. Exp. Med.* 142, 1263–1282.

Isberg, R. R., Voorhis, D. L., and Falkow, S. (1987). Identification of invasin: a protein that allows enteric bacteria to penetrate cultured mammalian cells. *Cell* 50, 769–778.

Kaparakis, M., Turnbull, L., Carneiro, L., Firth, S., Coleman, H. A., Parkington, H. C., Le Bourhis, L., Karrar, A., Viala, J., Mak, J., Hutton, M. L., Davies, J. K., Crack, P. J., Hertzog, P. J., Philpott, D. J., Girardin, S. E., Whitchurch, C. B., and Ferrero, R. L. (2010). Bacterial membrane vesicles deliver peptidoglycan to NOD1 in epithelial cells. *Cell. Microbiol.* 12, 372–385.

Kwok, T., Backert, S., Schwarz, H., Berger, J., and Meyer, T. F. (2002). Specific entry of *Helicobacter pylori* into cultured gastric epithelial cells via a zipper-like mechanism. *Infect. Immun.* 70, 2108–2120.

Liu, H., Rahman, A., Semino-Mora, C., Doi, S. Q., and Dubois, A. (2008). Specific and sensitive detection of *H. pylori* in biological specimens by real-time RT-PCR and in situ hybridization. *PLoS ONE* 3, e2689. doi:10.1371/journal.pone.0002689

Lundin, A., Nilsson, C., Gerhard, M., Andersson, D. I., Krabbe, M., and Engstrand, L. (2003). The NudA protein in the gastric pathogen *Helicobacter pylori* is an ubiquitous and constitutively expressed dinucleoside polyphosphate hydrolase. *J. Biol. Chem.* 278, 12574–12578.

Luo, Y., Liu, Y., Sun, D., Ojcius, D. M., Zhao, J., Lin, X., Wu, D., Zhang, R., Chen, M., Li, L., and Yan, J. (2011). InvA protein is a Nudix hydrolase required for infection by pathogenic *Leptospira* in cell lines and animals. *J. Biol. Chem.* 286, 36852–36863.

Maki, H., and Sekiguchi, M. (1992). MutT protein specifically hydrolyses a potent mutagenic substrate for DNA synthesis. *Nature* 355, 273–275.

Mitchell, S. J., and Minnick, M. F. (1995). Characterization of a two-gene locus from *Bartonella bacilliformis* associated with the ability to invade human erythrocytes. *Infect. Immun.* 63, 1552–1562.

Necchi, V., Candusso, M. E., Tava, F., Lunetti, O., Ventura, U., Fiocca, R., Ricci, V., and Solcia, E. (2007). Intracellular, intercellular and stromal invasion of gastric mucosa, preneoplastic lesions, and cancer by *H. pylori*. *Gastroenterology* 132, 1009–1023.

Noach, L. A., Rolf, T. M., and Tytgat, G. N. (1994). Electron microscopic study of association between *Helicobacter pylori* and gastric and duodenal mucosa. *J. Clin. Pathol.* 47, 699–704.

Olivero, O. A., Semino, C., and Poirier, M. C. (1990). Localization of DNA adducts induced by N-acetoxy-N-2-acetylaminofluorene in Chinese hamster ovary cells using electron microscopy and colloidal gold. *Genes Chromosomes Cancer* 2, 130–136.

Papadogiannakis, N., Willen, R., Carlen, B., Sjostedt, S., Wadstrom, T., and Gad, A. (2000). Modes of adherence of *Helicobacter pylori* to gastric surface epithelium in gastroduodenal disease: a possible sequence of events leading to internalisation. *APMIS* 108, 439–447.

Schneider, S., Weydig, C., and Wessler, S. (2008). Targeting focal adhesions: *Helicobacter pylori*-host communication in cell migration. *Cell Commun. Signal.* 6, 2.

Semino-Mora, C., Doi, S. Q., Marty, A., Simko, V., Carlstedt, I., and Dubois, A. (2003). Intracellular and interstitial expression of *Helicobacter pylori* virulence genes in gastric precancerous intestinal metaplasia and adenocarcinoma. *J. Infect. Dis.* 187, 1165–1177.

Tan, S., and Berg, D. E. (2004). Motility of urease-deficient derivatives of *Helicobacter pylori*. *J. Bacteriol.* 186, 885–888.

Tanner, V. A., Ploug, T., and Tao-Cheng, J. H. (1996). Subcellular localization of SV2 and other secretory vesicle components in PC12 cells by an efficient method of preembedding EM immunocytochemistry for cell cultures. *J. Histochem. Cytochem.* 44, 1481–1488.

Tomb, J. F., White, O., Kerlavage, A. R., Clayton, R. A., Sutton, G. G., Fleischmann, R. D., Ketchum, K. A., Klenk, H. P., Gill, S., Dougherty, B. A., Nelson, K., Quackenbush, J., Zhou, L., Kirkness, E. F., Peterson, S., Loftus, B., Richardson, D., Dodson, R., Khalak, H. G., Glodek, A., McKenney, K., Fitzegerald, L. M., Lee, N., Adams, M. D., Hickey, E. K., Berg, D. E., Gocayne, J. D., Utterback, T. R., Peterson, J. D., Kelley, J. M., Cotton, M. D., Weidman, J. M., Fujii, C., Bowman, C., Watthey, L., Wallin, E., Hayes, W. S., Borodovsky, M., Karp, P. D., Smith, H. O., Fraser, C. M., and Venter, J. C. (1997). The complete genome sequence of the gastric pathogen *Helicobacter pylori*. *Nature* 388, 539–547.

Viala, J., Chaput, C., Boneca, I. G., Cardona, A., Girardin, S. E., Moran, A. P., Athman, R., Mémet, S., Huerre, M. R., Coyle, A. J., DiStefano, P. S., Sansonetti, P. J., Labigne, A., Bertin, J., Philpott, D. J., and Ferrero, R. L. (2004). Nod1 responds to peptidoglycan delivered by the *Helicobacter pylori* cag pathogenicity island. *Nat. Immunol.* 5, 1166–1174.

Wang, Y. H., Wu, J. J., and Lei, H. Y. (2009). The autophagic induction in *Helicobacter pylori*-infected macrophage. *Exp. Biol. Med. (Maywood)* 234, 171–180.

Conflict of Interest Statement: The authors declare that the research was conducted in the absence of any commercial or financial relationships that could be construed as a potential conflict of interest.

Received: 01 November 2011; accepted: 01 February 2012; published online: 01 March 2012.

Citation: Liu H, Semino-Mora C and Dubois A (2012) Mechanism of H. pylori intracellular entry: an in vitro study. Front. Cell. Inf. Microbio. ***2****:13. doi: 10.3389/fcimb.2012.00013*